ORIGINAL

CrossMark

Comparison of aldehyde emissions simulation with FTIR measurements in the exhaust of a spark ignition engine fueled by ethanol

Paola Helena Barros Zarante[1] · José Ricardo Sodré[2,3]

Abstract

This work presents a numerical simulation model for aldehyde formation and exhaust emissions from ethanol-fueled spark ignition engines. The aldehyde simulation model was developed using FORTRAN software, with the input data obtained from the dedicated engine cycle simulation software AVL BOOST. The model calculates formaldehyde and acetaldehyde concentrations from post-flame partial oxidation of methane, ethane and unburned ethanol. The calculated values were compared with experimental data obtained from a mid-size sedan powered by a 1.4-l spark ignition engine, tested on a chassis dynamometer. Exhaust aldehyde concentrations were determined using a Fourier Transform Infrared (FTIR) Spectroscopy analyzer. In general, the results demonstrate that the concentrations of aldehydes and the source elements increased with engine speed and exhaust gas temperature. The measured acetaldehyde concentrations showed values from 3 to 6 times higher than formaldehyde in the range studied. The model could predict reasonably well the qualitative experimental trends, with the quantitative results showing a maximum discrepancy of 39% for acetaldehyde concentration and 21 ppm for exhaust formaldehyde.

1 Introduction

Ethanol is an interesting alternative fuel for spark ignition engines, as it can improve fuel economy and reduce carbon monoxide (CO), hydrocarbons (HC) and oxides of nitrogen (NO_X) emissions [1]. However, the incomplete combustion of ethanol produces high concentrations of aldehydes (RCHO) in the engine exhaust [2]. Aldehydes are highly reactive organic compounds that participate in complex chemical reactions in the atmosphere. Only the aldehydes encountered in the gaseous state are considered pollutants in internal combustion engines: formaldehyde (HCHO) and acetaldehyde (CH_3CHO). The emissions of aldehydes are higher for ethanol

fuel due to the presence of the hydroxyl functional group (OH), which is absent in gasoline [3].

Experiments conducted in a flexible fuel spark ignition engine showed that hydrous ethanol addition to gasoline with 25% v/v of anhydrous ethanol reduced CO and total HC, but increased carbon dioxide (CO_2), unburned ethanol and aldehyde emissions [4]. The results obtained from a spark ignition engine fueled with hydrous ethanol with up to 40% water content showed that increasing load decreased HC, formaldehyde and acetaldehyde emissions [5]. Benzaldehyde, acetaldehyde, formaldehyde and volatile organic compounds (VOCs) are the dominant emission products from bioethanol, similarly to ethanol–gasoline blends [6]. Formaldehyde emission from an ethanol fueled single cylinder engine was observed to be slightly lower in comparison with gasoline, but acetaldehyde emission was much higher [7].

From experiments in a spark ignition engine fueled by 5% of ethanol in gasoline (E5), 15% of ethanol in gasoline (E15), 5% of methanol in gasoline (M5) and 15% of methanol in gasoline (M15), higher exhaust concentrations of unburned ethanol and formaldehyde were found for E15 [8]. M15 emitted higher concentrations of methanol and formaldehyde, and acetaldehyde was not detected for M5 and M15 blends. Exhaust unburned ethanol was shown to be easier to eliminate than methanol in a vehicle three-way catalyst, while formaldehyde and acetaldehyde were eliminated with approximately

✉ José Ricardo Sodré
ricardo.sodre@bcu.ac.uk; ricardo@pucminas.br

Paola Helena Barros Zarante
paolabarros@hotmail.com

[1] Department of Mechanical Engineering, Universidad del Atlántico, Km 7 - Antigua vía Puerto Colombia, Barranquilla, Colombia

[2] Department of Mechanical Engineering, Pontifical Catholic University of Minas Gerais, Av. Dom José Gaspar, 500, Belo Horizonte, MG 30535-901, Brazil

[3] School of Engineering and the Built Environment, Birmingham City University, Millenium Point, Curzon St, Birmingham B4 7XG, UK

🖄 Springer

equal efficiency [9]. Carbonyl species, including acetaldehyde and formaldehyde, are heavily dependent on engine operation and combustion mode, as noted by comparing spark ignition and homogeneous charge compression ignition [10].

In the European Union (EU) regulations, all carbon compounds measured with the FID (Flame Ionization Detector) analyzer is treated as hydrocarbon emissions, while, in the United States of America (USA), alcohols and aldehydes are measured and reported separately from hydrocarbons [11]. In Brazil, the alcohol part can be measured separately on voluntary basis. The FID sensitivity was higher at the detector temperature of 113 °C, as stated by the USA Emissions Prevent Association (EPA) when testing alcohol fueled vehicles, than at 190 °C, often used as default setting in the EU. The standardized method approved in the USA to analyze aldehyde emissions is FTIR (Fourier-Transform Infrared) spectroscopy, and, in Brazil, HPLC (High-Performance Liquid Chromatography). For both methods the sample should be taken in DNPH (2,4-dinitrophenyl hydrazine) cartridges.

Detailed kinetic models were developed by different authors [12–14] to describe the chemical reactions occurring during ethanol combustion. These models simulate the chemical reactions within reactors used for combustion studies. However, they exhibit great chemical complexity, requiring several hundreds of reactions to reach the results. The kinetic mechanism in one of those models contains 107 chemical species and 568 reactions in order to simulate formaldehyde formation accurately [15]. Other models presented elsewhere for ethanol combustion include from 43 to 135 chemical species [16, 17]. From a 47-species model applied to an ethanol fueled engine, methane (CH_4) emission was found at higher concentration than ethane (C_2H_6), both participating on aldehyde formation [18]. Acetaldehyde and formaldehyde were found in significant quantity, the former higher showing higher concentration.

The intermediate temperature heat release of an engine has been examined using a simulation model [19], based on detailed chemistry for ethanol combustion previously described elsewhere [12]. A quasi-dimensional engine simulation code was used to predict the gas dynamics, combustion and knock occurrence in alcohol engines [20]. An in-house developed model with detailed chemical kinetic mechanism of methanol and ethanol combustion and consideration to formaldehyde and acetaldehyde has satisfactorily reproduced fuel decay as well as major and intermediate species profiles [21].

This paper presents a quasi-dimensional model of formaldehyde and acetaldehyde formation to simulate exhaust concentrations of a spark ignition engine fueled by gasoline or ethanol. Differently from the previous models here reviewed, the current model calculates the rate of formation of aldehydes from chemical reactions of methane, ethane and unburned ethanol oxidation, formed as intermediate products of ethanol combustion. This approach is expected to lead to much faster

calculations. The results from the simulation are compared with experimental data from laboratory tests in a production vehicle, with exhaust aldehydes being measured by FTIR spectroscopy.

2 Aldehyde formation mechanism

The chemical kinetics reaction mechanism of aldehyde formation from in-cylinder ethanol combustion that serve as a basis to the simulation model is explained next. The aldehydes formed in the intermediate stages of the combustion process are immediately consumed by the flame front due to the high temperature attained in the combustion chamber. The aldehyde formation reactions here described take place during the post-flame oxidation process of the unburned fuel, starting in the cylinder and propagating through the exhaust pipe. In order to calculate the exhaust aldehyde concentration, the oxidation reactions are considered separately, being the final concentration given by the sum of the parts produced in each reaction.

The exhaust acetaldehyde (CH_3CHO) is mainly formed in the intermediate phase of the post-flame oxidation of unburned ethanol (CH_3CH_2OH), according to [22]:

$$CH_3CH_2OH + \frac{1}{2}O_2 \rightarrow CH_3CHO + H_2O \tag{1}$$

The rate of acetaldehyde formation from ethanol oxidation is developed from the reaction equation described by Eq. (1), and is given by [22]:

$$\frac{d[CH_3CHO]}{dt}$$
$$= A \cdot T^n \cdot \exp\left(\frac{-E_A}{\overline{R} \cdot T}\right) \cdot \frac{7,200}{\left(\overline{R} \cdot T\right)^{1/2}} \cdot \exp\left(\frac{-69,090}{T}\right) \cdot [O_2]^{1/2} \cdot [CH_3CH_2OH] \tag{2}$$

where constants A and E_A assume the values of 1.12×10^{13} cm³/gmol.s and 127.3 kJ/gmol, respectively [22]. The unit of measure for acetaldehyde formation rate given by Eq. (2) is gmol/cm³.s.

Acetaldehyde is also formed from the post-flame oxidation process of ethane (C_2H_6), which is generated when the decomposition process of unburned fuel in the exhaust gas is stopped at an intermediate stage of the chemical reaction. The interruption is mainly due to reduction of temperature and oxygen concentration. The first product of ethane oxidation is ethanol (Eq. (3)), which is subsequently oxidized by the oxygen present to produce acetaldehyde as given by Eq. (1) [22]:

$$C_2H_6 + \frac{1}{2}O_2 \rightarrow C_2H_5OH \tag{3}$$

The mathematical model that represents the rate of formation of acetaldehyde from ethane oxidation is written as [22]:

$$\frac{d[CH_3CHO]}{dt}$$
$$= A \cdot T^n \cdot \exp\left(\frac{-E_A}{\overline{R} \cdot T}\right) \cdot \frac{7,200}{\left(\overline{R} \cdot T\right)^{1/2}} \cdot \exp\left(\frac{-69,090}{T}\right) \cdot [O_2]^{1/2} \cdot [C_2H_6]$$

$$(4)$$

where constants A and E_A assume the values of 3.98×10^{13} cm^3/gmol.s and 213.0 kJ/gmol, respectively [22]. The unit of measure for acetaldehyde formation rate given by Eq. (4) is gmol/cm^3.s.

Similar to acetaldehyde formation from ethane, formaldehyde is originated from methane (CH_4) formed during the post-flame oxidation of unburned ethanol. The first product of methane oxidation is methanol (CH_3OH), which is immediately oxidized to formaldehyde in the presence of oxygen remaining [22]:

$$CH_4 + \frac{1}{2}O_2 \rightarrow CH_3OH \qquad\qquad (5)$$

$$CH_3OH + \frac{1}{2}O_2 \rightarrow HCHO + H_2O \qquad (6)$$
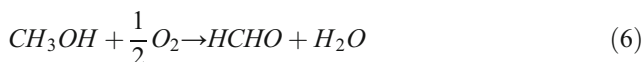
Therefore, the formation rate of formaldehyde from methane oxidation takes the form [22]:

$$\frac{d[HCHO]}{dt}$$
$$= A \cdot T^n \cdot \exp\left(\frac{-E_A}{\overline{R} \cdot T}\right) \cdot \frac{7,200}{\left(\overline{R} \cdot T\right)^{1/2}} \cdot \exp\left(\frac{-69,090}{T}\right) \cdot [O_2]^{1/2} \cdot [CH_4]$$

$$(7)$$

where A is the pre-exponential factor of Arrhenius (6.46×10^{14} cm^3/gmol.s) [14], T is the temperature (K), n is the temperature exponent, E_A is the reaction activation energy (179.9 kJ/gmol) [12], and $\overline{R}$ is the universal gas constant (8.31434×10^{-3} kJ/gmol.K) [22].

3 Methodology

3.1 Numerical simulation

The differential equations of the chemical reactions in the cylinder and the exhaust pipe are time-integrated, obtaining algebraic expressions for the final concentrations of methane, ethane formaldehyde and acetaldehyde. Aldehyde formation is calculated from the combustion chamber to the sampling point in the exhaust pipe. While the concentration of unburned ethanol is given by the commercial software AVL BOOST [23], the concentrations of methane, ethane, formaldehyde and acetaldehyde are calculated by a FORTRAN-based aldehyde emission model

from the reaction equations presented by Marinov [12] and Costa et al. [22]. The calculation is performed through the exhaust process.

The AVL BOOST software was used to simulate the cycle of an ethanol-fueled, four-stroke, spark ignition engine, with focus to produce complementary data to aldehyde simulation. The software offers two possibilities for gas composition modeling: the classical species transport and the general species transport. The software calculates the gas properties in time steps, giving instant composition. For the current simulation, the general species transport module was used to present a larger amount of exhaust species. The composition of the gas can be described based on an arbitrary number of species that are defined directly by the user. The minimum number of species is 7: fuel, O_2, N_2, CO_2, H_2O, CO and H_2. For each species a mass fraction conservation equation is solved with each of the model elements.

The flow in the pipes is treated by the software as one-dimensional. This means that pressures, temperatures and flow velocities obtained from the solution of the gas dynamic equations represent mean values over the cross-section of the pipes [24]. The input data for the simulation correspond to the engine used in the experiments performed to compare with the model. Figures 1 and 2 shows a schematics of the simulated engine.

The AVL BOOST simulation reproduced the engine test conditions applied in the experiments. The tests were performed at engine crankshaft speeds of 2000, 3000, 4000 and 5000 rpm. From this simulation the temperature, pressure, oxygen concentration and unburned ethanol concentration were obtained inside the cylinder and in the exhaust pipe. The input data for the simulation are shown in Table 1. As the software is not able to calculate aldehyde emissions, the calculated cylinder temperature and pressure diagrams throughout the cycle and the exhaust concentrations of oxygen and unburned ethanol were used as input data for a model developed to calculate aldehyde emissions in FORTRAN code.

The model built in FORTRAN uses the chemical reaction equations to calculate the concentrations of ethane, methane and unburned ethanol within the cylinder for subsequent calculation of the concentrations of formaldehyde and acetaldehyde in the cylinder and exhaust pipe. The exhaust pipe concentrations of ethane, methane and unburned ethanol were also calculated by the model. The simulation was performed varying the engine speed, and the input parameters provided by the AVL BOOST simulation software is shown by Table 2. The flowchart of the numerical simulation algorithm is shown by Fig. 1, and includes the following steps:

- Reading data of crankshaft speed, cylinder and exhaust temperatures and pressures, oxygen and ethanol mass fraction from the AVL BOOST software.

Fig. 1 Flowchart of the aldehyde model
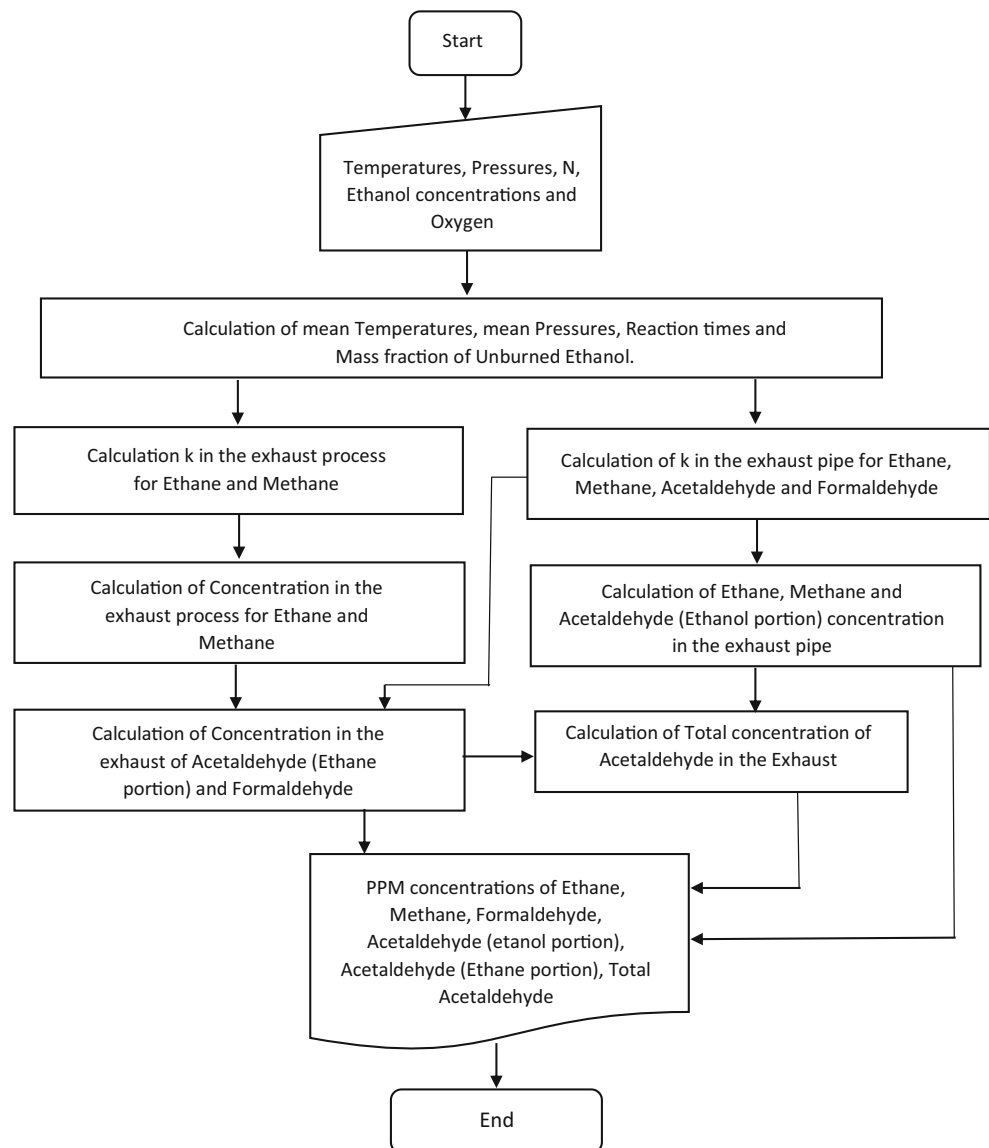
- Calculation of total number of moles, reaction time and mass fraction of unburned ethanol.
- Calculation of Arrhenius constants for methane, ethane, formaldehyde and acetaldehyde.
- Calculation of the concentrations of methane and ethane.
- Calculation of formaldehyde and acetaldehyde from the calculated values of methane, ethane and unburned ethanol.
- Calculation of the total aldehyde concentration.

3.2 Experiments

The model results were compared with experimental data obtained from a 4-cylinder, 1.4-l, FIAT FIRE Flex model spark ignition engine. The engine also featured 10.35:1 compression ratio, 60 kW rated power, 121 N.m rated torque, and was operated in a bench test dynamometer, fueled with hydrous ethanol (6.8% wt./wt. of water). K-type thermocouples, with uncertainty of reading of ±2 °C, were installed in the engine to measure the intake air temperature and the exhaust gas temperature. The exhaust gas sample was taken from the exhaust pipe, close to the exhaust port, and driven through a heated sampling line into a FTIR analyzer, to avoid condensation of heavy components. The measurements were made with the engine operating at steady state condition, wide open throttle, air/fuel equivalence ratio 0.96, variable load and crankshaft speeds of 2000, 3000, and 4000 rpm, with corresponding ignition timings of 25.7 crankshaft degrees before top dead center (°BTDC), 29.3°BTDC and 27.9°BTDC, respectively. The results shown in the following section are the average of three tests performed at each engine operating condition.

Fig. 2 Schematic diagram of simulated engine in AVL BOOST
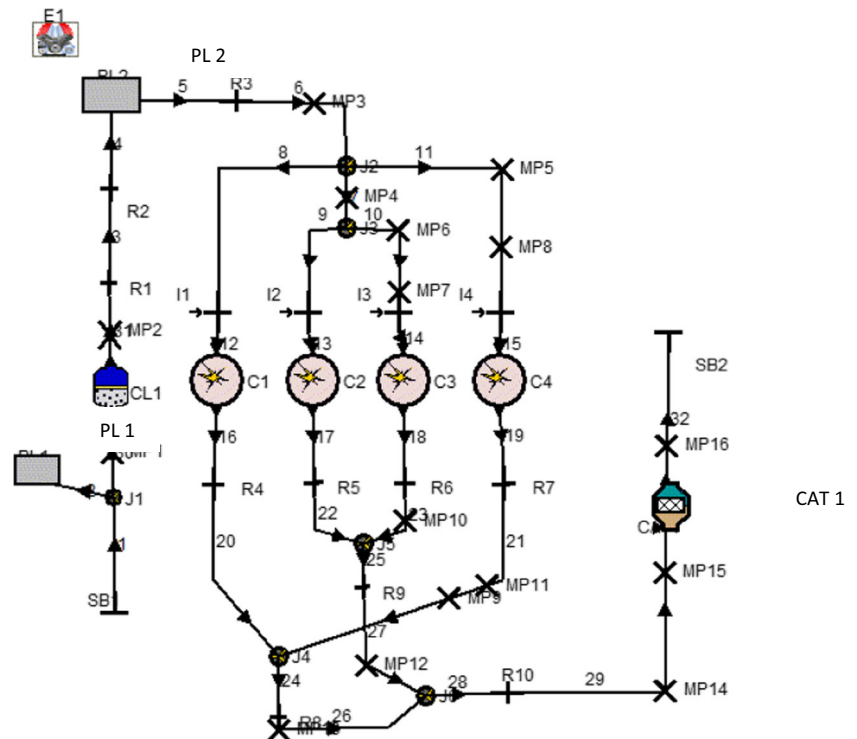
4 Results and discussion

The results from the simulation are compared with experimental values measured by Fourier Transform Infrared spectroscopy (FTIR). The concentrations of formaldehyde, acetaldehyde and their main producers – methane, ethane and unburned ethanol – were measured. Acetaldehyde corresponds to the sum of the parts formed from the post-flame oxidation of unburned ethanol and ethane. All substances present a trend of increased concentration with increasing engine speed, as it can be seen in Figs. 3, 4, 5, 6 and 7. Model and experiments generally show qualitative agreement, while the proximity of the quantitative values depends on the engine operating condition.

The general trends obtained for formaldehyde and acetaldehyde, shown in Figs. 3 and 4, are in agreement with Amaral and Sodré [24, 25] and Pang et al. [26], who also found increased aldehyde concentration with engine speed. It is

observed that the concentrations of measured and simulated acetaldehyde are larger than those of formaldehyde, as found by Amaral and Sodré [24] using ethanol as fuel, and by Pang et al. [26], He et al. [27], and Song et al. [28], who used ethanol-gasoline blends. The acetaldehyde concentration levels found by Amaral and Sodré [24, 25] are close to the one found in the present work (Fig. 4).

The increase of formaldehyde (Fig. 3) and acetaldehyde (Fig. 4) concentrations with engine speed is due to the increase of exhaust gas temperature with engine speed (Fig. 8) [16], together with the increase of the concentrations of methane (Fig. 5), ethane (Fig. 6) and unburned ethanol (Fig. 7), as it can be inferred from Eqs. (4), (5) and (7). The increase of exhaust gas temperature with engine speed (Fig. 8) is due to the shorter time for the engine cycle to be completed, making combustion finish later in the cycle. Thus, when the exhaust valve opens the burned gas temperature in the cylinder is higher. The exhaust gas temperature and the concentrations of methane, ethane and unburned ethanol are the main factors that affects

Table 1 AVL BOOST software input data

Parameter	Value or specification
Number of simulated cycles	50
Bore × stroke (mm)	72 × 84
Compression ratio	10.35:1
Air/fuel ratio	12
Fuel	Ethanol
Crankshaft speed (rpm)	2000, 3000, 4000 and 5000

Table 2 FORTRAN software input data

Data calculated by the AVL BOOST software	
Temperature (K)	Start of the exhaust process
Pressure (KPa)	End of exhaust process
	Sampling point
Molar concentration	Oxygen
	Unburned ethanol

Fig. 3 Simulated and measured (FTIR) concentrations of exhaust formaldehyde
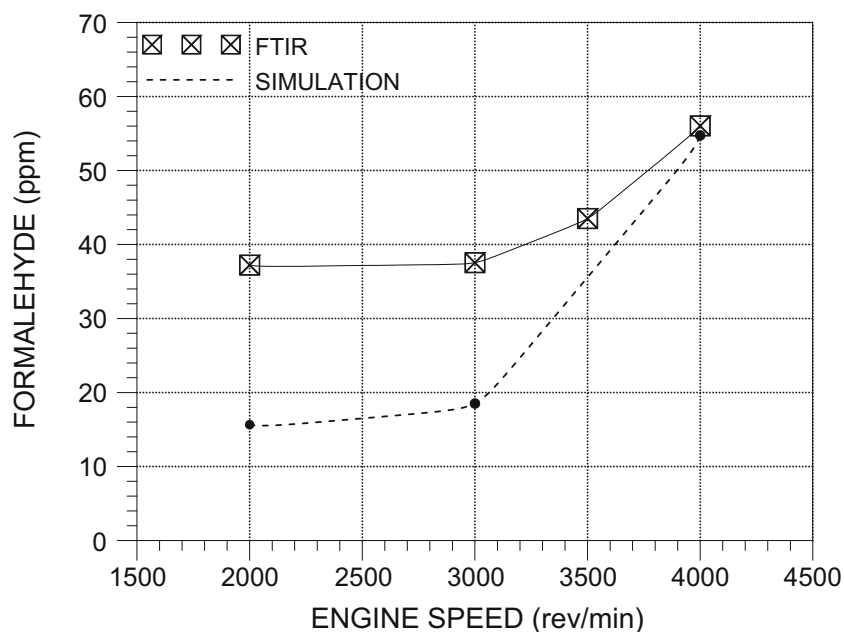
aldehyde formation. Increasing gas temperature and the concentrations of those components accelerates the post-flame oxidation reactions that originate formaldehyde and acetaldehyde (Eqs. (4), (5) and (7)).

The trends obtained for methane measured by FTIR analysis and numerical simulation (Fig. 5) resemble those found for the measured and simulated formaldehyde (Fig. 3), of which methane is the main producer. The simulated values of formaldehyde underestimate the measured values in the whole range investigated, showing the largest discrepancy at 2000 rpm, of 58% (Fig. 3). This is a direct consequence from the simulated values of methane also underestimate the measured values in the whole speed range (Fig. 5), once

formaldehyde is formed from the methane oxidation process (Eqs. (4) to (5)). However, the quantitative difference at that condition is of only 21 ppm, which is a very small amount. The underestimation of methane concentration by the model may be due to non-consideration of methane formation from breakdown reactions of heavier hydrocarbons formed during ethanol burn.

The simulated and measured concentrations of exhaust ethane have trend resemblance and close quantitative values in all the speed range studied (Fig. 6). The exhaust ethane concentration at any speed much higher than those of methane (Fig. 5) and unburned ethanol (Fig. 7), the other source elements of aldehydes. It has previously been reported that

Fig. 4 Simulated and measured (FTIR) concentrations of exhaust acetaldehyde
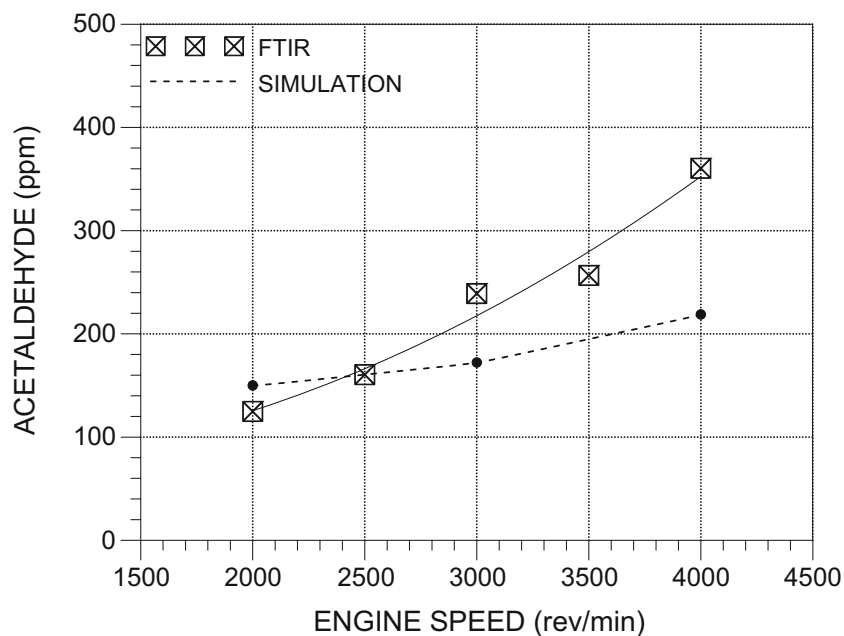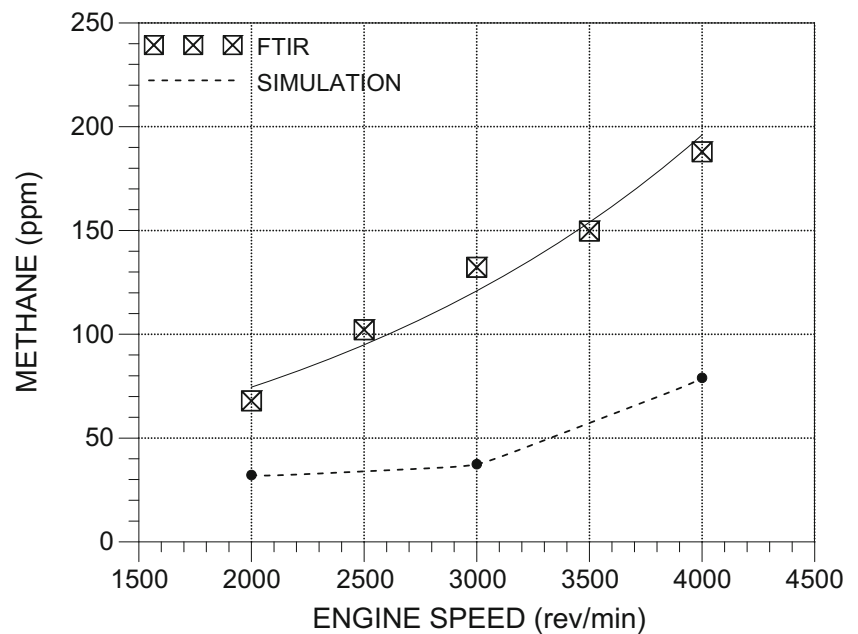
Fig. 5 Simulated and measured (FTIR) concentrations of exhaust methane

acetaldehyde formation from ethane is very small in comparison with the amounts produced from unburned ethanol, of the order of 10^4 to 10^5 lower [22]. Therefore, it is not main responsible to determine the qualitative trend and the quantitative levels of exhaust acetaldehyde (Fig. 4).

In order to increase the engine speed a higher amount of fuel is injected in the engine and, with increasing engine speed, combustion becomes more inefficient because of the shorter period it is allowed for completion and the lesser amount of air admitted by cycle. This is the reason why the exhaust ethanol concentration is increased with engine speed, as shown by Fig. 7. The increased concentration of unburned

ethanol (Fig. 7) together with higher exhaust gas temperature (Fig. 8) are responsible for the higher amounts of methane (Fig. 5) and ethane (Fig. 6) with increasing engine speed, as these components are intermediate products of the post-flame oxidation of the unburned fuel.

From Fig. 7, it is observed that the simulated ethanol concentrations have closed proximity to the measured values obtained by FTIR, except at 4000 rev/min, when a maximum discrepancy of 17% was recorded. At this condition the shorter cycle time may not be enough for combustion completion, thus producing an increase of unburned fuel that is not followed by the model. The trend shown by exhaust unburned

Fig. 6 Simulated and measured (FTIR) concentrations of exhaust ethane
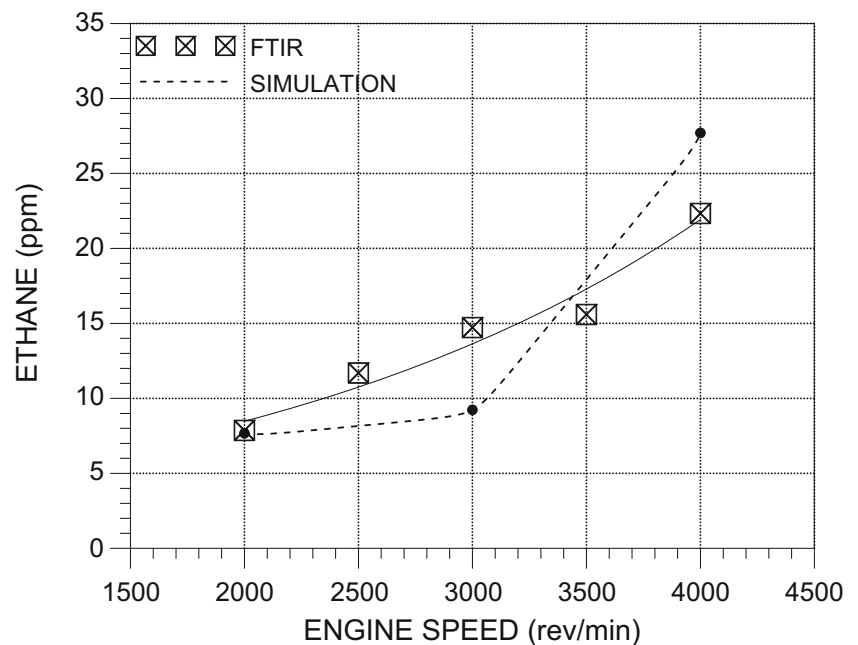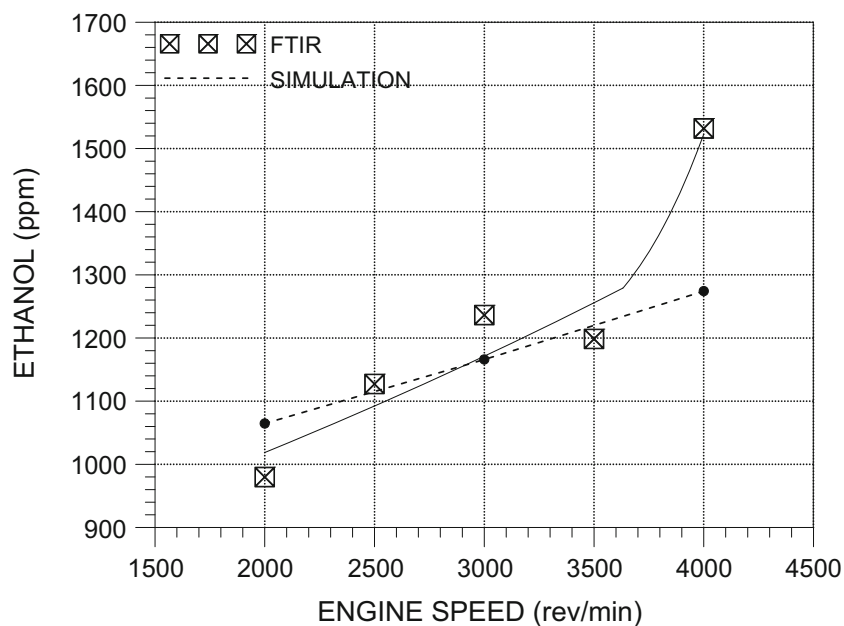
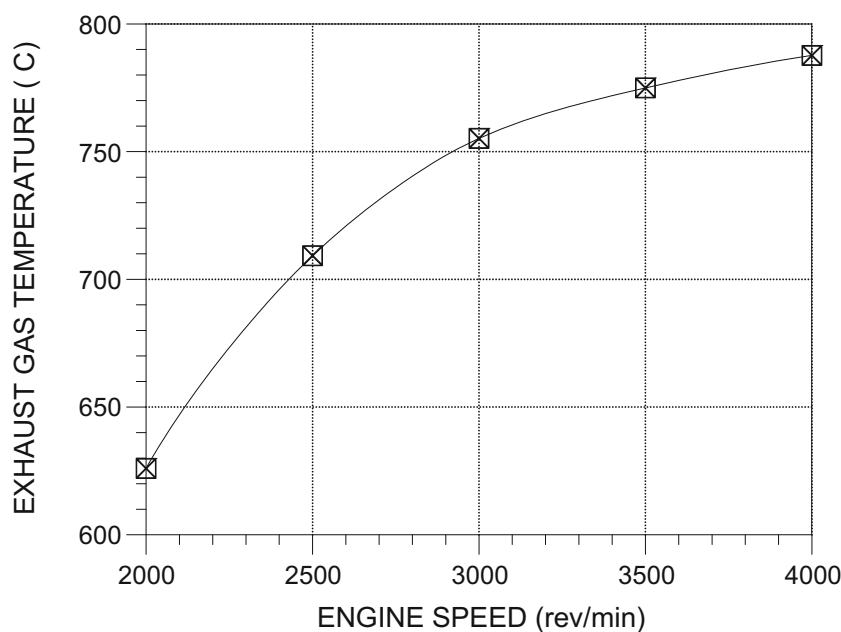**Fig. 7** Simulated and measured (FTIR) concentrations of exhaust unburned ethanol

ethanol resembles that of acetaldehyde (Fig. 4), as unburned ethanol is its main source element. The studies of Vourliotakis et al. [21] and Amaral and Sodré [25] confirm these results, also associating the increase of unburned ethanol concentration to the increase of acetaldehyde concentration.

5 Conclusions

The simulated values of exhaust formaldehyde, acetaldehyde and their main producers – methane, ethane and unburned ethanol – present a general trend agreement with the measured values by FTIR analysis, all showing increased concentrations

with increasing engine speed. These trends observed for formaldehyde and acetaldehyde were explained by the increase of their source elements and exhaust gas temperature with increasing engine speed, which accelerates the oxidation rates of aldehyde formation reactions. The simulated and measured values of formaldehyde presented the highest discrepancy of 58% at the engine speed of 2000 rev/min and exhaust gas temperature of 626°C, but this corresponded to a quantitative difference of only 21 ppm. The maximum discrepancy found between the simulated results and the measured data for exhaust acetaldehyde of 17% at the engine speed of 4000 rev/min and exhaust gas temperature of 788°C. The simulation model was proven to be a useful tool to estimate exhaust

Fig. 8 Variation of exhaust gas temperature with engine speed

formaldehyde and acetaldehyde from an ethanol-fueled engine.

References

1. Keating E (1993) Applied combustion. Marcel Dekker, New York
2. Ghadikolaei M (2016) Effect of alcohol blend and fumigation on regulated and unregulated emissions of IC engines—a review. Renew Sust Energ Rev 57:1440–1445. https://doi.org/10.1016/j.rser.2015.12.128
3. Basshuysen R, Schäfer F (2004) Internal combustion engine handbook: basics, components, systems, and perspectives. SAE International, Warrendale
4. Melo T, Machado G, Belchior C, Colaço M, Barros J, Oliveira E, Oliveira D (2012) Hydrous ethanol–gasoline blends – combustion and emission investigations on a flex-fuel engine. Fuel 97:796–804. https://doi.org/10.1016/j.fuel.2012.03.018
5. Munsin R, Laoonual Y, Jugjai S, Imai Y (2013) An experimental study on performance and emissions of a small SI engine generator set fuelled by hydrous ethanol with high water contents up to 40%. Fuel 106:586–592. https://doi.org/10.1016/j.fuel.2012.12.079
6. Manzetti S, Andersen O (2014) A review of emission products from bioethanol and its blends with gasoline. Background for new guidelines for emission control. Fuel 140:293–301. https://doi.org/10.1016/j.fuel.2014.09.101
7. Wang C, Xu H, Daniel R, Ghafourian A, Herreros J, Shuai S, Ma X (2013) Combustion characteristics and emissions of 2-methylfuran compared to 2,5-dimethylfuran, gasoline and ethanol in a DISI engine. Fuel 103:200–211. https://doi.org/10.1016/j.fuel.2012.05.043
8. Agarwal A, Shukla P, Gupta J, Patel C, Prasad R, Sharma N (2015) Unregulated emissions from a gasohol (E5, E15, M5, and M15) fuelled spark ignition engine. Appl Energy 154:732–741. https://doi.org/10.1016/j.apenergy.2015.05.052
9. Bielaczyc P, Woodburn J, Klimkiewicz D, Pajdowski P, Szczotka A (2013) An examination of the effect of ethanol–gasoline blends' physicochemical properties on emissions from a light-duty spark ignition engine. Fuel Process Technol 107(2013):50–63. https://doi.org/10.1016/j.fuproc.2012.07.030
10. Hasan A, Abu-jrai A, Al-Muhtaseb A, Tsolakis A, Xu H (2016) Formaldehyde, acetaldehyde and other aldehyde emissions from HCCI/SI gasoline engine equipped with prototype catalyst. Fuel 175:249–256. https://doi.org/10.1016/j.fuel.2016.02.005
11. Sandstroem-Dahl C, Erlandsson L, Gasste J, Lindgren M (2010) Measurement methodologies for hydrocarbons, ethanol and aldehyde emissions from ethanol fuelled vehicles. SAE Int 2010:01–1557
12. Marinov N (1999) A detailed chemical kinetic model for high temperature ethanol oxidation. In J Chem Kinet 31:183–220. https://doi.org/10.1002/(SICI)1097-4601(1999)31:3<183::AID-KIN3>3.0.CO;2-X
13. Li J, Kazakov A, Chaos M, Dryer F (2007) Chemical kinetics of ethanol oxidation. In: Western States Section of the Combustion Institute (ed) Proceedings of the 5th US Combustion Meeting, San Diego
14. Frassoldati A, Cuoci A, Faravelli T, Niemann U, Ranzi E, Seiser R, Seshadri K (2010) An experimental and kinetic modeling study of n-propanol and iso-propanol combustion. Combust Flame 157:2–16. https://doi.org/10.1016/j.combustflame.2009.09.002
15. Dias V, Duynslaegher C, Contino F, Vandooren J, Jeanmart H (2012) Experimental and modeling study of formaldehyde combustion in flames. Combust Flame 159:1814–1820. https://doi.org/10.1016/j.combustflame.2012.01.006
16. Viggiano A, Magi V (2012) A comprehensive investigation on the emissions of ethanol HCCI engines. Appl Energy 93:277–287. https://doi.org/10.1016/j.apenergy.2011.12.063
17. Viggiano A, Magi V (2014) Dynamic adaptive chemistry applied to homogeneous and partially stratified charge CI ethanol engines. Appl Energy 113:848–863. https://doi.org/10.1016/j.apenergy.2013.08.002
18. Maurya R, Akhil N (2016) Numerical investigation of ethanol fuelled HCCI engine using stochastic reactor model. Part 2: parametric study of performance and emissions characteristics using new reduced ethanol oxidation mechanism. Energy Convers Manag 121:55–70. https://doi.org/10.1016/j.enconman.2016.03.076
19. Vuilleumier D, Korzarac D, Mehl M, Saxena S, Pitz W, Dibble R, Chen J-Y, Sarathy S (2014) Intermediate temperature heat release in an HCCI engine fueled by ethanol/n-heptane mixtures: an experimental and modeling study. Combust Flame 161:680–695. https://doi.org/10.1016/j.combustflame.2013.10.008
20. Vancoillie J, Sileghem L, Verhelst S (2014) Development and validation of a quasi-dimensional model for methanol and ethanol fueled SI engines. Appl Energy 132:412–425. https://doi.org/10.1016/j.apenergy.2014.07.046
21. Vourliotakis G, Skevis G, Founti M (2015) Some aspects of combustion chemistry of C1–C2 oxygenated fuels in low pressure premixed flames. Proc Combust Inst 35:437–445. https://doi.org/10.1016/j.proci.2014.06.060
22. Costa T, Zarante P, Sodré J (2013) Simulation of aldehyde formation in ethanol fuelled spark ignition engines. In: Sens M, Baar R (eds) Engine processes. Expert Verlag, Berlin
23. AVL BOOST V2010 (2010) Users Guide. AVL List GmbH, Austria
24. Amaral R, Sodré J (2002) Influence of engine operating parameters on aldehyde emissions from an ethanol-fueled vehicle. Combust Sci Technol 174:153–165. https://doi.org/10.1080/00102200208984091
25. Amaral R and Sodré J (2001) Aldehyde emissions from an ethanol-fuelled vehicle as influenced by engine geometric parameters. In: SAE International (ed) General emissions research and development (SP1631), SAE 2001–01-1998, SAE Inc, Warrendale, pp 29–34. https://doi.org/10.4271/2001-01-1998.
26. Pang X, Um Y, Yuan J, He H (2008) Carbonyls emission from ethanol-blended gasoline and biodiesel-ethanol-diesel used in engines. Atmos Environ 42:1349–1358. https://doi.org/10.1016/j.atmosenv.2007.10.075
27. He B-Q, Shuai S-J, Wang J-X, He H (2003) The effect of ethanol blended diesel fuels on emissions from a diesel engine. Atmos Environ 37:4965–4971. https://doi.org/10.1016/j.atmosenv.2003.08.029
28. Song C, Zhao Z, Liv G, Song J, Liu L, Zhao R (2010) Carbonyl compound emissions from a heavy-duty diesel engine fueled with diesel fuel and ethanol–diesel blend. Chemosphere 79:1033–1039. https://doi.org/10.1016/j.chemosphere.2010.03.061